A Cu_{20} Cluster-Based Moisture-Absorbent Composite Membrane for Efficient Photocatalytic Hydrogen Evolution in Seawater under Non-Contact Configuration

Longfei Chao, Chunhui Zhang, Jie Wang, Lixiao Song, Yundong Cao*, Jiayuan Zhang, Hong Liu*, Yihai Song, GuangGang Gao*

School of Materials Science and Engineering

University of Jinan

Jinan 250022, China.

*Corresponding authors

E-mail: mse_caoyd@ujn.edu.cn (Yundong Cao); mse_liuh@ujn.edu.cn (Hong Liu); mse_gaogg@ujn.edu.cn (Guanggang Gao)

Materials

The metal precursors $Cu(COOCH_3)_2 \cdot H_2O$ (98 mol%, Sigma-Aldrich) and copper powder (Aladdin), NH_4VO_3 (99 mol%, Macklin) were used without further purification. Ethinylestradiol ligand was purchased from Macklin. Polyvinyl Alcohol (PVA) was purchased from Aladdin. The seawater comes from the Bohai Sea.

Characterization methods

A Nicolet 6700 spectrophotometer was used to record the FTIR spectra with KBr as the phragmoid auxiliary material. Powder X-ray diffraction (XRD) was performed using X-ray diffraction (XRD, Rigaku SmartLab 9KW) with Cu Kα radiation. Data was recorded for the 2θ range from 5° to 80° in steps of 0.05° using an integration time of 1 s. The morphology of the synthesized nanomaterials was analyzed by scanning electron microscope instrument (SEM, Zeiss, Gemini 300) and energy-dispersive X-ray spectroscopy (EDX, Oxford, X-Max^N 50) analysis was performed using the SEM to provide elemental composition information. A CEL-SPH2N photo catalysis system was used to obtain performance of hydrogen evolution reaction. A CHI660E electrochemical workbench was carried out to obtain electrochemical performance. UV-Vis diffuse reflectance spectra were measured using Shimazu UV-visible spectrophotometer UV-8000. The Fl emission spectra was detected by a shimadzu fluorescence spectrophotometer RF-6000 with the excitation wavelength at 255 nm. Detailed processes of electrochemical measurement are shown in the supplementary data.

The apparent quantum efficiency (AQE)

The apparent quantum efficiency (AQE) were calculated under different single-wavelength light using Equation (1):

$$AQE = \frac{2 \times the\ number\ of\ evolved\ H2\ molecules}{the\ number\ of\ incident\ photons} \times 100\% \quad (1)$$

Electrochemical tests

A CHI660E electrochemical workbench was carried out to determine the electrochemical performance. A three-electrode system was used to record the electrochemical data, in which a glassy carbon electrode was used as the working electrode, a platinum wire as the counter electrode, and an Ag/AgCl electrode as the reference electrode. A 0.1 M sodium sulfate solution was used as an electrolyte solution. The preparation of the working electrode was as follows: 5 mg of catalyst was added into the system of water (650 μL), Nafion (50 μL) and Isopropyl alcohol (350 μL) before ultrasonic dispersion for 30 min. Afterwards, the resultant mixture (5 μL) was dried on the surface of glassy carbon.

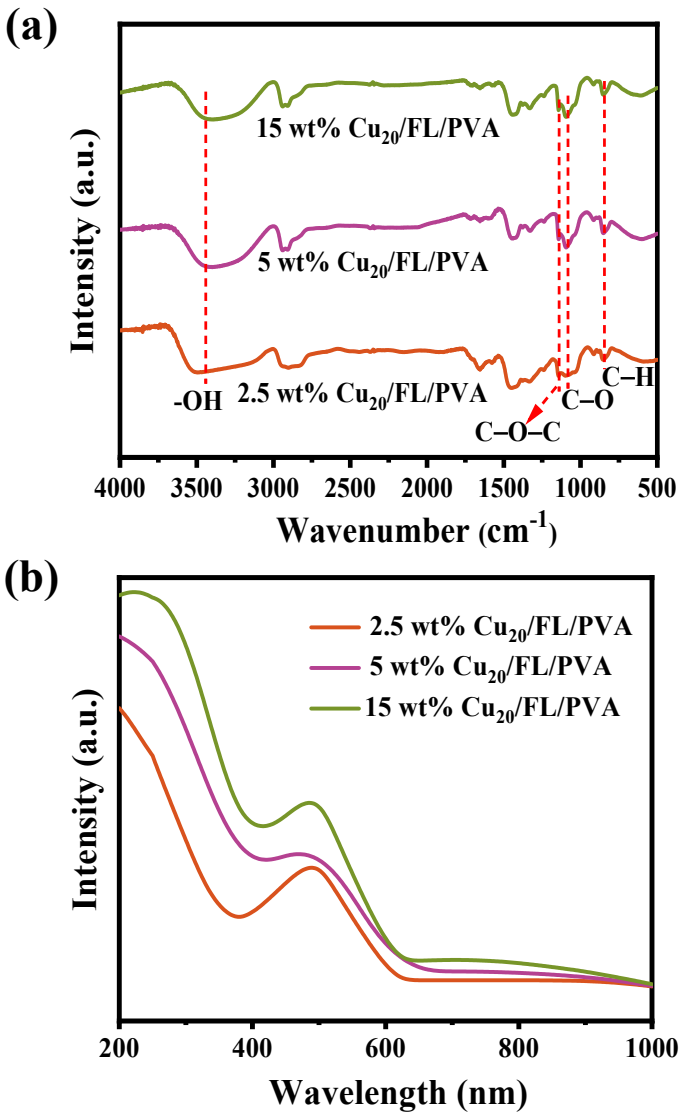

Fig. S1 (a) FT-IR spectra of membranes with 2.5 wt% Cu_{20}/FL/PVA, 5 wt% Cu_{20}/FL/PVA, 15 wt% Cu_{20}/FL/PVA; (b) UV-Vis diffuse reflectance spectra of membranes with 2.5 wt% Cu_{20}/FL/PVA, 5 wt% Cu_{20}/FL/PVA, 15 wt% Cu_{20}/FL/PVA.

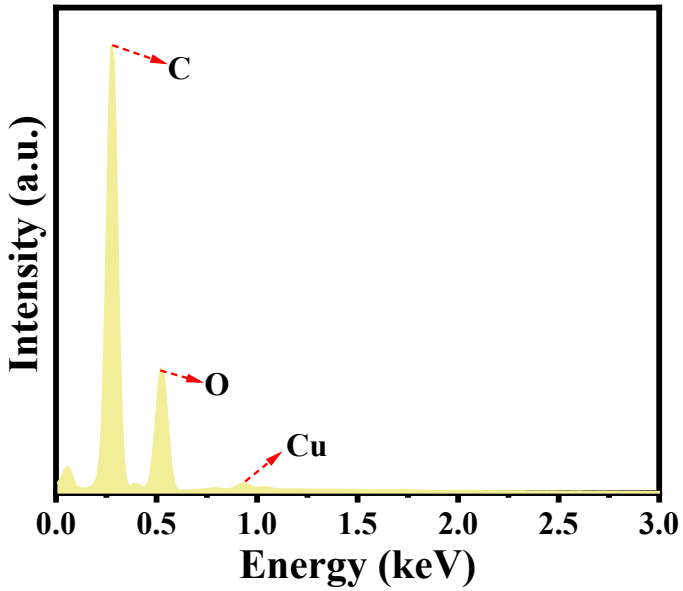

Fig. S2 Element distribution map of 10 wt% Cu_{20}/FL/PVA composite membrane.

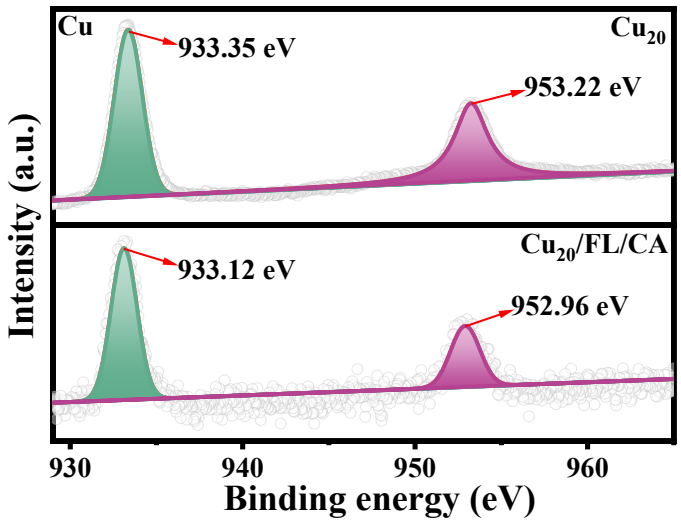

Fig. S3 Cu 2p XPS spectra of Cu_{20} and Cu_{20}/FL/PVA composite.

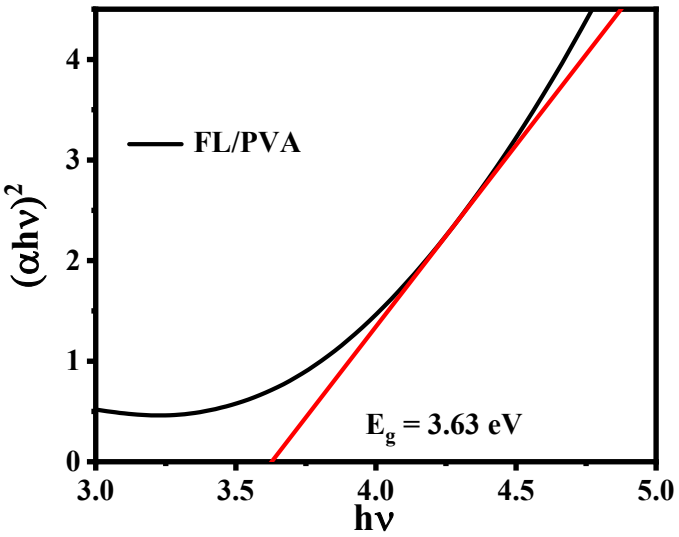

Fig. S4 Optical band gap of the FL/PVA membrane calculated from the UV-Vis DRS data.

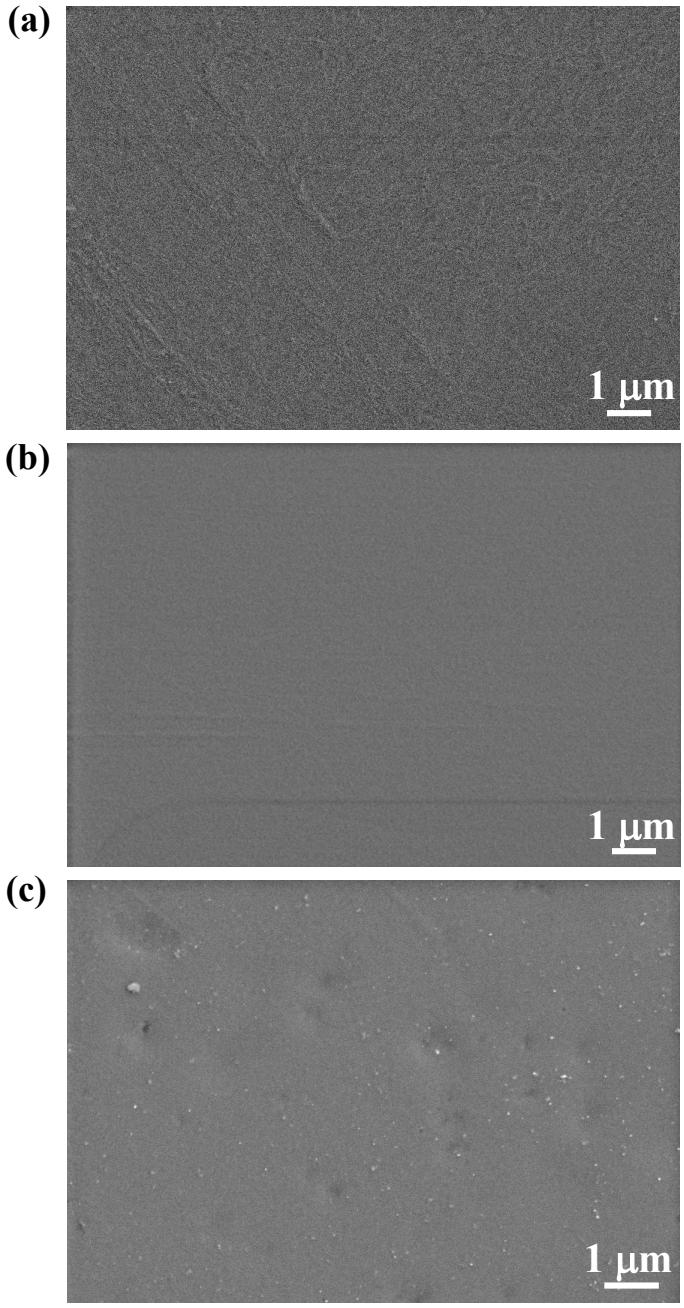

Fig. S5 SEM image of the PVA (a), FL/PVA (b) and 15 wt% Cu_{20}/FL/PVA (c) membrane.

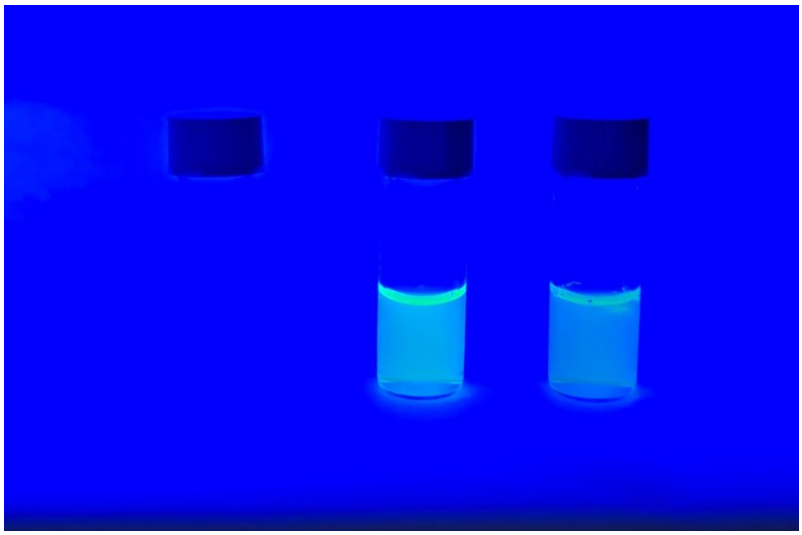

Fig. S6 Photoluminescence images of pristine PVA, FL/PVA, and Cu_{20}/FL/PVA composite membranes under ultraviolet light irradiation.

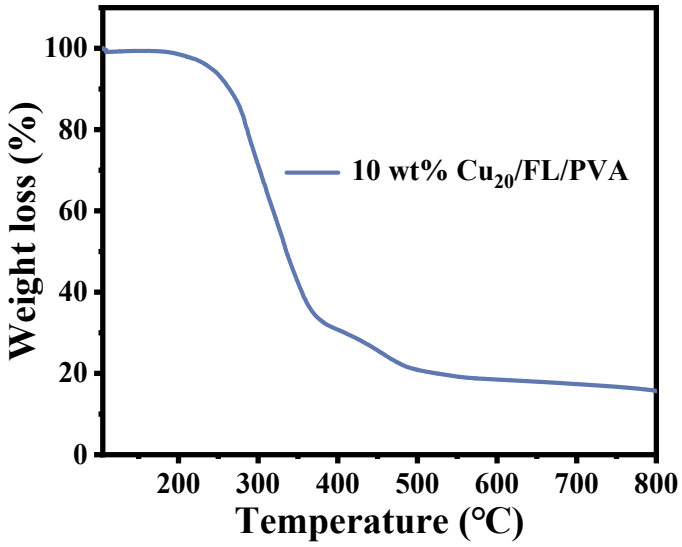

Fig. S7 Thermogravimetric analysis of 10 wt% Cu_{20}/FL/PVA membrane under N_2 atmosphere.

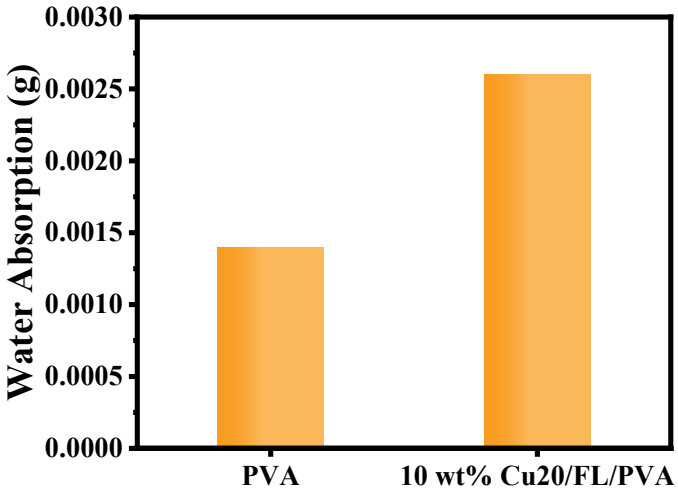

Fig. S8 Water absorption performance test of the original PVA film and the 10 wt% Cu_{20}/FL/PVA composite film under humid conditions.

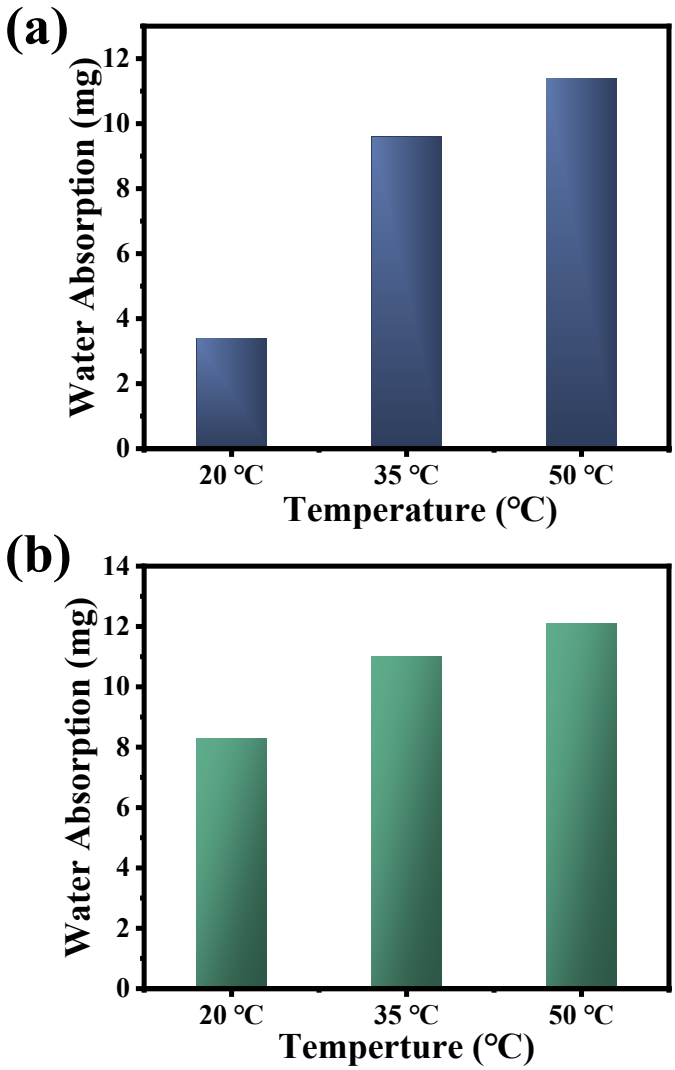

Fig S9 Water absorption properties of 10 wt% Cu_{20}/FL/PVA composite membrane in deionized water (a) and seawater (b) at different temperatures.

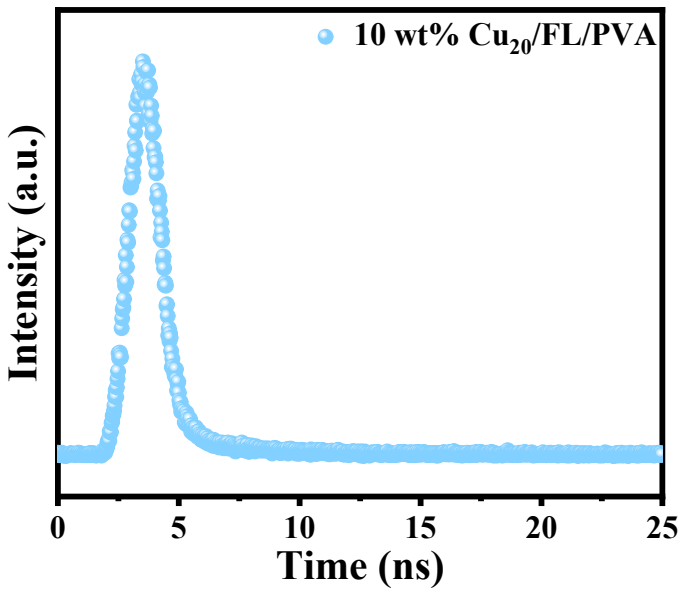

Fig. S10 Time-resolved transient PL decay spectra of Cu_{20}/FL/PVA, λ_{ex} = 280 nm.

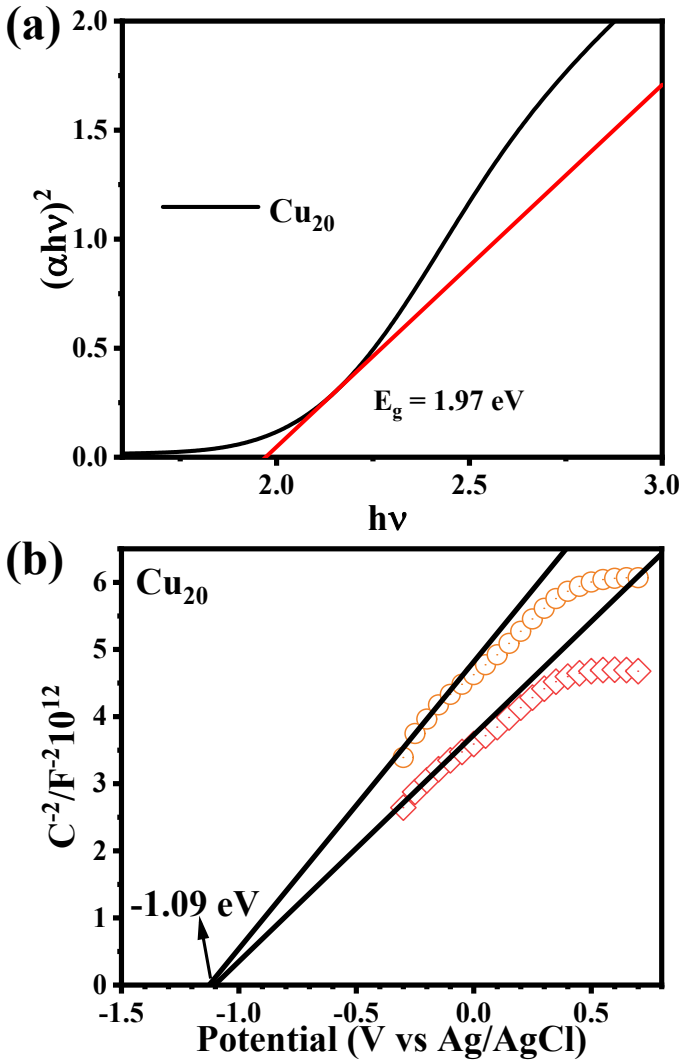

Fig. S11 (a) HOMO-LUMO energy gap of the Cu_{20} membrane calculated from the UV-Vis DRS data; (b) Mott-Schottky curve of Cu_{20}.

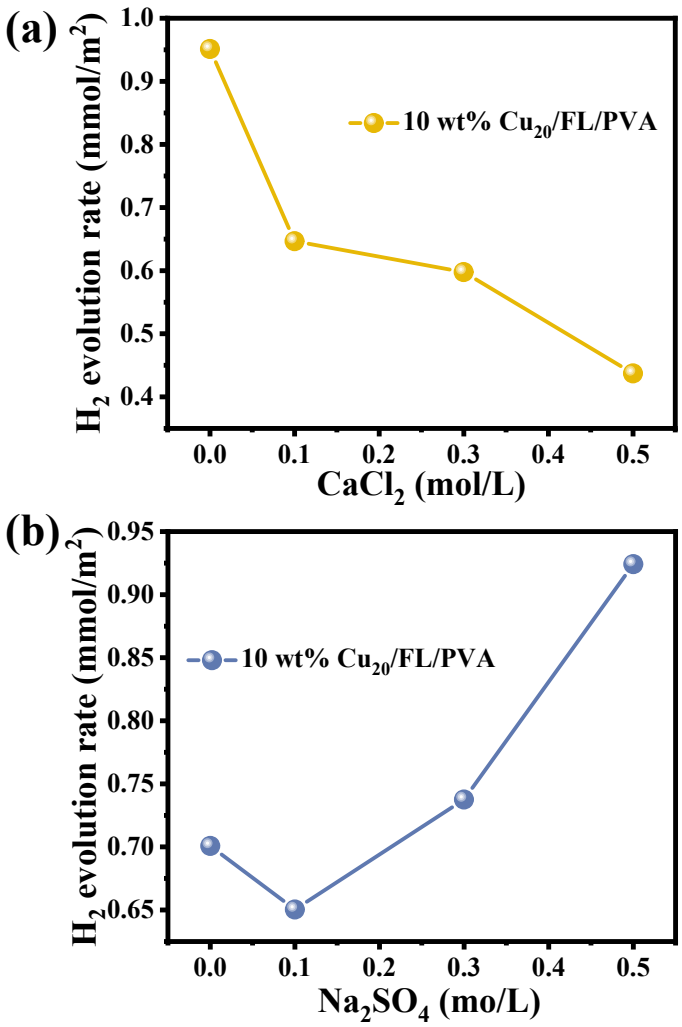

Fig. S12 Photocatalytic hydrogen generation rate of 10 wt% Cu_{20}/FL/PVA in (a) $CaCl_2$ and (b) Na_2SO_4 solutions with varying concentrations.

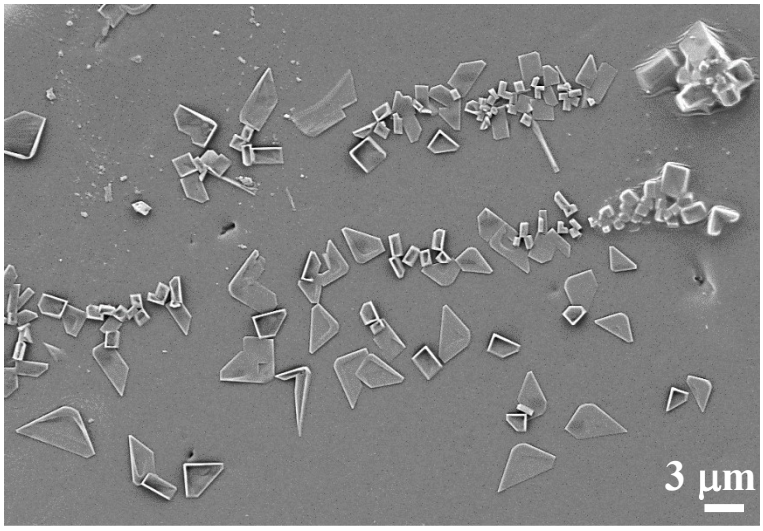

Fig. S13 SEM morphology of membrane surface after photocatalytic reaction in seawater system.

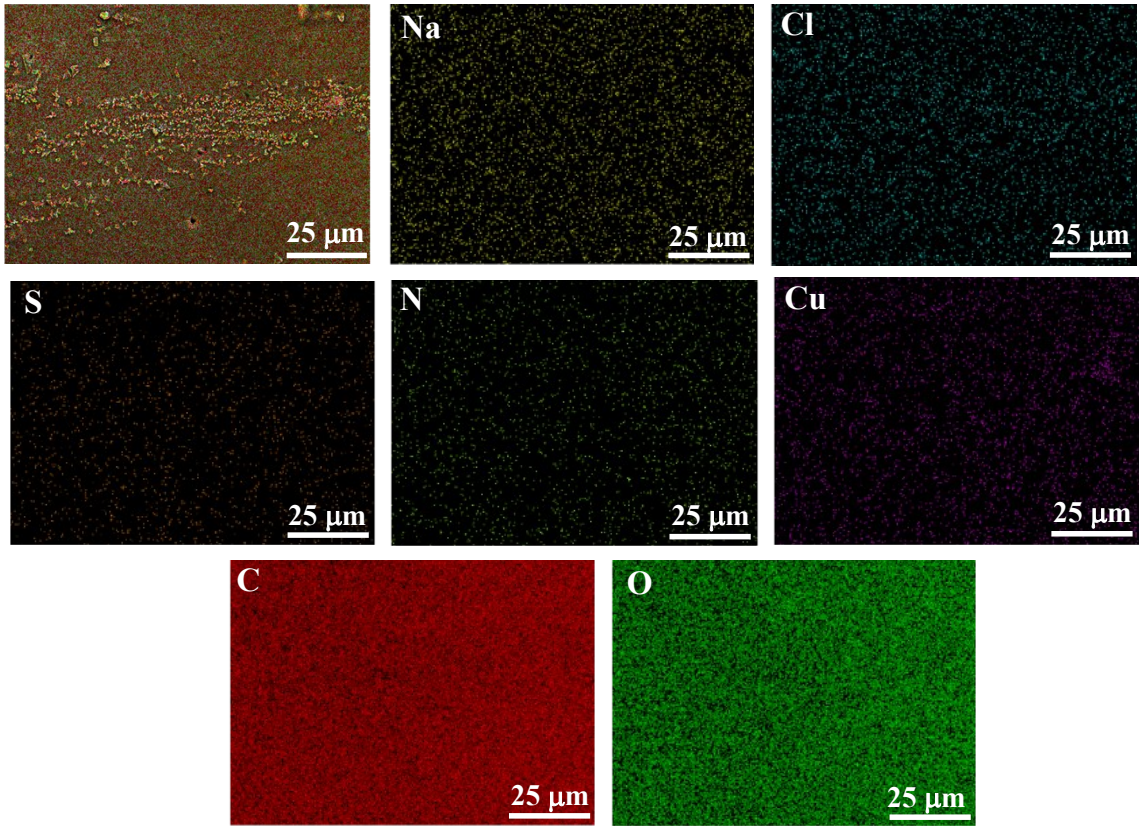

Fig. S14 Element distribution map of membrane surface after photocatalytic reaction in seawater system.

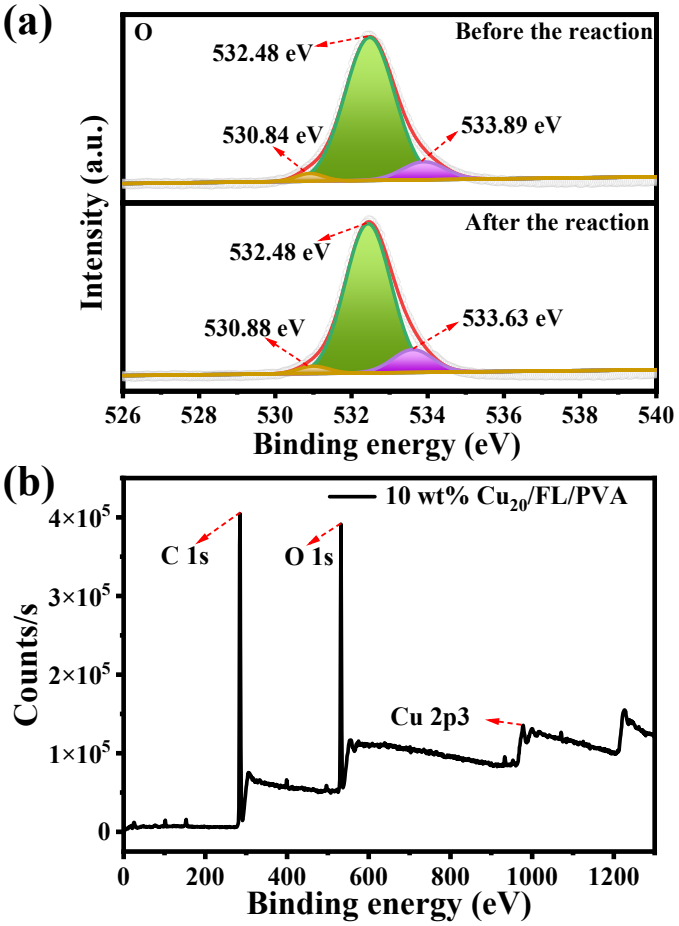

Fig. S15 (a) O XPS spectra before and after photocatalysis; (b) 10 wt% Cu_{20}/FL/PVA's XPS spectra of survey.

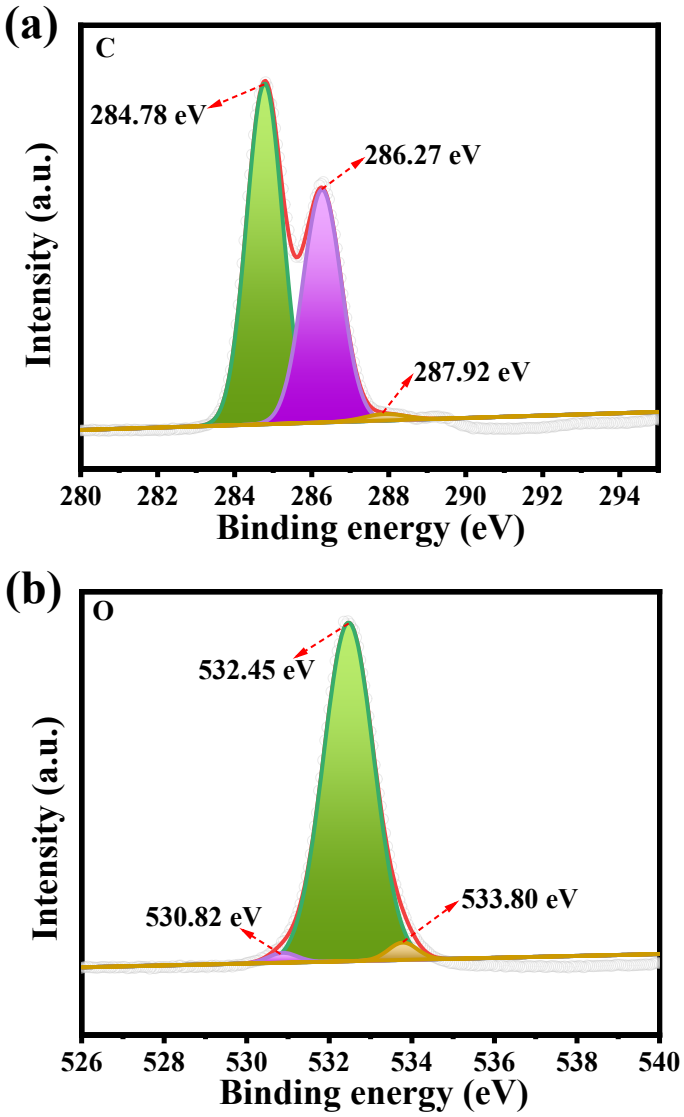

Fig. S16 XPS spectra of the FL/PVA composite membrane: (a) C 1s and (b) O 1s.

Table S1 Comparative analysis of this study with existing literature reports.

Sample	Preparation method	Sacrificial agent	H2 evolution rate	Refence
Cu_{20}/FL/PVA	Scraping method	/	1.46 mmol/m^2	This work
PVA/Pt/NT/STO	Scraping and soaking	Methanol	34895 μmol/h/g	(1)
THPP-sg-PSf/TiO2	Nonsolvent -induced phase separation method	TEOA	9.74 mmol/m^2	(2)
PVA-ZnOS	Freezing-induced gelation	Na_2S/Na_2SO_3 aqueous solution	18.8 μmol/h	(3)
ZIS/PAN	Freezing-induced gelation	TEOA	1836 μmol/g/h	(4)
M-CuZn	Inversion method	/	90.07 μmolg/h	(5)
PS-PNS-PVP	Scraping method	Methanol	6419 μmol/h/g	(6)
BOC-CNF@CNT	/	TEOA	25.42 μmol/g/h	(7)

Notes and references

1 J. Lee and M. Wey, *J. Colloid Interface Sci.*, 2020, 573, 158-164.

2 Y. Chen, M. Wang, F. Yan, Y. Zhang, L. Dong, L. Wang, Z. Cui and J. Li, *Appl. Surf. Sci.*, 2021, 566, 150667.

3 V. Poliukhova, W. Lei, S. Khan, E. L. Tae, N. Suzuki, C. Terashima A. Fujishima, K. Katsumata and S. Cho, *Catalysts*, 2022, 12, 272.

4. Y. Zhang, L. Niu, Z. Li, T. Yang, Y. Liu and Z. Kang, *Appl. Catal. B Environ. Energy*, 2024, 357, 124300.

5. P. García-Ramírez, L.A. Diaz-Torres, S. J. Castaneda-Palafox, M. Villagomez-Mora, E. Avalos-Marr and R. Lopez Gonzalez, *Int. J. Hydrogen Energy*, 2024, 79, 943-951.

6. J. Lee, Y. Chang and M. Wey, *Int. J. Hydrogen Energy*, 2021, 46, 11597-11606.

7. W. Zhou, H. Huang, Y. Wu, J. Wang, Y. Yamauchi, J. Kim, S. M. Osman, X. Xu, L, Wang, C. Wang and Z. Yuan, *Chem. Eng. J.*, 2023, 471, 144395.